The influence of ultrasonic pre-treatments on metal adsorption properties of softwood-derived biochar

Aneeshma Peter[a], Bruno Chabot[a], Eric Loranger[a*]

[a] I2E3 – Institut d'Innovations en Écomatériaux, Écoproduits et Écoénergies, à base de biomasse, Université du Québec à Trois-Rivières, 3351, boul. des Forges, Trois-Rivières, Québec, Canada G8Z 4M3

* Corresponding author:

Tel: +1 819 376-5011, poste 4518

Fax: +1 819 376-5148

E-mail: Eric.Loranger1@uqtr.ca

Abstract

Biomass-derived biochars are studied extensively because of their unique surface properties and efficiency in removing heavy metals from aqueous solution. Power ultrasound pre-treatments is interesting in this context, as they can make significant changes in the physicochemical characteristics of biomass. Herein, we studied their effect on adsorption characteristics of softwood biochar under different conditions of frequency, power, temperature and exposure time of ultrasound. The 40 kHz pre-treated samples exhibited around 26 to 52 percent increase in equilibrium adsorption capacity (Q_e) which highly depends on the combination of power versus time and temperature of ultrasound. The isotherm and thermodynamic studies also showed that the mechanical effect of ultrasound

plays a vital role in enhancing the surface. Results from this study demonstrated that ultrasound pre-treatment conditions influence the behaviour of biochar towards metal adsorption and ultrasonic pre-treatments can be used as an efficient processing method for biomass residues and the derived products.

Keywords: Biochar, ultrasonic pre-treatments, metal adsorption, adsorption capacity, surface modification

1. Introduction

Biochar is a solid residue obtained from thermochemical conversion of biomass in an oxygen-limited environment (Manyà, 2012). Due to the similar physical appearance, biochars are often misinterpreted with charcoal and other carbonised materials, which mainly are thermal residues after complete combustion of feedstocks. The basic difference being the source material, which is mostly fresh residual matter in case of biochar rather than fossilized or good quality biomass in other carbonised materials. This carbon-rich, semi-crystalline, porous material has emerged as an alternate to activated carbons in recent decades because of the unique characteristics such as good specific surface area, surface functionality, easy availability and low-cost processability (Oliveira et al., 2017). Efficient removal of contaminants from industrial effluent popularised the material among the existing adsorption techniques (Mohan et al., 2014, Tan et al., 2015, Inyang et al., 2016).

The properties of wood derived biochar have been extensively studied during recent decades, especially in Quebec (Canada), because of the abundance of forest trees, which are mostly softwoods. Different research policies have been adopted to facilitate and enhance the properties of softwood derived biochar, since the physical as well as the chemical properties are highly dependent on feedstock type, production methods, pre and post processing of feedstocks and reaction conditions involving temperature, pressure, residence time, etc (Nartey and Zhao, 2014). Y. Sun et al., (2014) explored the effect of temperature, production method and feedstock type on the physicochemical and biological properties of different biochars and showed that production method and feedstock type have high influence on the properties. Mukome et al., (2013) also studied the trend of feedstock type on biochar

properties. They have analysed biochar from twelve different feedstocks and stated that physical and chemical properties vary depending on the feedstock type. The properties of wood derived biochar have been studied extensively. The main factor which affects the physical and chemical properties of these biochars are the pyrolysis temperature and difference in content of cellulose, hemicellulose and lignin (Jindo et al., 2014; Chowdhury et al., 2016; Behazin et al., 2016). For example, in a study by Shasha et al., (2017) the physicochemical properties of different varieties of hard and softwood were examined and showed that the properties are dependent on the pyrolysis temperature. They have also stated that the properties vary depending on the cellulose, hemicellulose and lignin content of the wood. Therefore, developing and optimising an efficient treatment method can be interesting for tuning the physicochemical properties of the material for the same feedstock and pyrolysis conditions.

Application of power ultrasound in biomass processing is a recently developed area. The invasive technique uses high intensity acoustic waves to change or modify the properties as well as promote chemical and thermal decomposition reactions within the material. The formation of cavitation bubbles followed by the microjet collision experienced during the bubble implosions were employed to expose inaccessible regions on the surface (Leong et al., 2011). Limited reports are available in literature that examine the effect of ultrasound for different biomass applications. Z. He et al., (2017) investigated the influence of ultrasonic pre-treatments on eucalyptus wood. They proved that the ultrasound can modify the physicochemical structure of the wood and can significantly increase the crystallinity of the material. Qui and co-workers (2016) demonstrated that ultrasound pre-treatments on

hardwood can increase its dimensional stability by chemical modification and it is an effective way to reduce water adsorption rate in wood. A recent study by Chatterjee et al., (2018) examined the effect of ultrasound cavitation induced physical activation to enhance the chemical modification of biochar for CO_2 sequestration. Sajjadi et al., (2019) also has demonstrated the physical modification of biochar by low frequency ultrasound to enhance the urea functionalisation, which enhances the adsorption capacity of the material. Recently, Cherpozat et al., (2017) has investigated the effect of ultrasonic pre-treatments on the pyrolysis biooils yield giving a significant progress in ultrasonic enhanced lab-scale pyrolysis and hence motivating the further investigation on the effect of ultrasonic pre-treatment in pyrolysis product characteristics.

In this study, we aim at investigating the ultrasonic pre-treatment effects on the overall structure of biochar and its adsorption behaviour. Proper understanding and controlling the structure-property relationship of biochar can improve its application in the field of heavy metal removal. It can also rectify the issues regarding material quality of post-consumer feedstocks and convert them into useable by-products. To the best of our knowledge, this is the first study to evaluate ultrasound pre-treatment effects on biomass and change in properties of biochar via systematic analysis methods.

2. Materials and Methods

2.1 Biochar production and characterisation

The biochar used in this project were obtained from lab-scale pyrolysis of softwood chips (mix of spruce, fir, pine and larch) provided by an eastern Canadian pulp and paper mill (Loranger et al., 2016). Ultrasonic treatments were performed in a 34 L ultrasonic bath,

model BT90 from Ultrasonic Power Corporation (USA), made of 316 L stainless steel, equipped with 12 transducers located below the bottom plate of the bath. Commercially available frequency generators of 40 and 170 kHz were used to produce between 250 and 1000 W of nominal ultrasonic energy to study the mechanical and sonochemical effects, respectively. The bath temperature was fixed at 20ºC and 80ºC and the exposure time was varied between 1 and 2 hours. The list of ultrasound pre-treatments is given in Table 1.

(Table 1 here)

pH of the material was measured using Accumet XL20, Thermo Fisher Scientific pH-meter in deionized water at 1:2 weight by volume ratio after stirred at room temperature for two hours. Zeta Potential of untreated and ultrasound pre-treated wood biochar was measured for a suspension of biochar powder in deionized water with pH 6.14 using Zetasizer-nano series from Malvern Instruments. The point zero charge was determined from the plot of pH against Zeta potential. Scanning Electron Microscopy (SEM) images were captured using Hitachi SU1510 instrument to understand the changes in biochar surface. Surface area was measured via the Brunauer, Emmett and Teller (BET) method that measures N_2 gas sorption (0.162 nm^2) at 77 K. Approximately 100 mg of biochar was outgassed at 200°C (16 hours) and then analysed on an Autosorb-1 Surface Area Analyzer (Quantachrome Instruments).

2.2 Cu (II) adsorption experiments

The metal adsorption experiments were performed using a batch equilibration technique. Stock solution (1000 ppm) of Cu (II) was prepared by dissolving analytical grade anhydrous $CuSO_4$ in deionized water. The pH of the copper solution ranged from 4.8 to 5. The kinetic experiments for all the biochar samples were conducted in 125 mL Erlenmeyer flask with 5

g/L biochar mixed in 100 ppm Cu (II) solution. The mixture was then agitated on a reciprocating shaker at room temperature (22 ± 2 ºC) at 150 rpm. Samples were taken at desired intervals and subsequently filtered with Whatman No. 1 filter paper. The filtrates were analysed for residual heavy metal concentration in the solution using EDTA titration described by Prasad and Raheem, (1992). The amount of adsorbed metal ions, Q (mg/g), was calculated using Eq. (1).

$$Q\ (\frac{mg}{g}) = \frac{(C_{initial} - C_{final})ppm * V(L)}{m\ (g)} \quad (1)$$

Experimental data were fitted to pseudo first order (Eq. (2)) and pseudo second order (Eq. (3)) kinetic models using the linear form of equations. Both of them are the commonly fitted kinetic models for metal adsorption on biochar. In most of the cases, heavy metal adsorption on biochar follows pseudo first or second order kinetics (Tan et al.,2015).

$$\log(Q_e - Q_t) = \log Q_e - \frac{k_1 * t}{2.303} \quad (2)$$

$$\frac{t}{Qt} = \frac{1}{k_2 * Qe^2} + \frac{t}{Q_e} \quad (3)$$

Where Q_t and Q_e (mg/g) are adsorbed metal amount at time t (minute) and equilibrium, k_1 and k_2 (g/mg. min) are the rate constants for pseudo first order and second order kinetic model, respectively. The best fit model was determined by regression factor R^2 to understand the mechanism of adsorbent-adsorbate interaction. Slope and intercept values were used to calculate Q_e and rate constant, k.

Adsorption isotherms for selected samples were obtained. During these experiments the initial Cu (II) concentrations varied from 10 to 200 ppm. To evaluate and compare the

adsorption capacities of Cu (II), linearized Langmuir and Freundlich models were used to fit the experimental data as they are the most commonly used and well fitted adsorption models for heavy metal adsorption on biochar. (Zhang et al., 2013; Jia et al., 2013; Chen et al., 2011).

The linear equations of the Freundlich and Langmuir adsorption models are expressed, respectively, by Eq. (4) and Eq. (5):

$$\log Q_e = \log K_f + \frac{1}{n}\log C_e \quad (4)$$

$$\frac{C_e}{Q_e} = \frac{1}{b*Q_{max}} + \frac{1}{Q_{max}} C_e \quad (5)$$

Where Q_e is the amount of the metal adsorbed per unit weight of biochar at equilibrium (mg/g), C_e is the equilibrium concentration of solution (mg/L). K_f and n are indicators of relative adsorption capacity and surface heterogeneity, respectively. Q_{max} is the maximum monolayer adsorption capacity (mg/g) and b the Langmuir constant related to the degree of adsorption affinity.

A dimensionless constant R_L calculated (Eq. 6) using Langmuir constant and initial concentration represents model fitness for a particular system (Ozcan et al., 2006; Brandes et al., 2019). If value of R_L falls between 0 and 1, the system is considered appropriate for adsorption purpose.

$$R_L = 1/ (1+b*C_i) \quad (6)$$

Where b is the Langmuir constant and C_i is the initial concentration. The favourability of the adsorption is identified by the value of R_L as given below:

$R_L > 1$, unfavourable

$R_L = 1$, linear

$0 < R_L < 1$, favourable

$R_L < 0$, irreversible

The temperature effect was assessed by equilibrating 0.1 g biochar with 20 mL Cu (II) solution on shaker at 25, 40, and 60 ºC. The thermodynamics of the adsorption processes were estimated using the following equations:

$$K_e = \frac{Q_e}{C_e} \quad (7)$$

$$\Delta G^0 = -RT\, lnK_e \quad (8)$$

$$\Delta G^0 = \Delta H^0 - T\Delta S^0 \quad (9)$$

$$lnK_e = \frac{\Delta S^0}{R} - \frac{\Delta H^0}{RT} \quad (10)$$

Where Q_e is the amount of the metal adsorbed per unit weight of biochar at equilibrium (mg/g), C_e is the equilibrium concentration of solution (mg/L), R is gas constant 8.314, T (K) absolute temperature and K_e (L/g) the equilibrium adsorption constant.

The values of enthalpy ΔH^0 and entropy ΔS^0 can be determined from the slope and intercept of the plot ln K_e vs 1/T. Gibb's free energy ΔG^0 can be obtained using Eq. (8) with the values of ΔH^0 and ΔS^0.

The statistical analysis of the kinetics data was performed using JMP Pro 14 (SAS) for the detailed investigation of ultrasound pre-treatment effects on equilibrium adsorption capacity

and rate constant k. Effect of each ultrasonic pre-treatment on the kinetics parameters is useful to determine the change in surface property of biochar with pre-treatments.

Kinetic experiment results were compared with commercially available carbon (Fluval Carbon for purifiers) to compare the adsorption per unit surface area. Equilibrium adsorption capacity was measured for activated carbon, untreated, UST-3 and UST-11 and the results were compared in terms of adsorption per unit surface area (mg/m^2).

3. Results and Discussions

The syntheses conditions and chemical characterisations of all biochar were done and reported before (Peter et al., 2019). The pyrolysis temperature was ranged between 510 to 580^oC. In brief, the chemical characteristics of ultrasound pre-treated, and untreated biochar remained same, confirming that the ultrasound had affected only on the physical morphology of biochar. The chemical composition of feedstock and biochar synthesised is summarised in Table 2. Almost 87 percent is carbonised with a 10-weight percent of oxygen present, which can be from carboxylic, phenolic lactonic surface functional groups. These functionalities can act as anchoring sites for the positively charged adsorbates.

(Table 2 here)

For adsorption experiments, at least 3 trials were performed, and the average value is reported. This is required considering the variations in experimental data because of the mixed feedstock softwoods, heterogeneity in structure and variations in effect of temperature inside pyrolysis reactor.

3.1 Ultrasound pre-treatment effects on biochar

The microscopic images of biochar prepared from wood chips after different ultrasonic conditions were studied to understand if there are any obvious surface morphology changes. The comparison of surface images has been done for all samples and Fig.1 represents few among them which are untreated and maximum and minimum conditions of ultrasound pre-treatments.

(Figure 1 here)

Unlike untreated wood biochar, in most of the ultrasonic conditions, the slit like channels on the wood surface were cleaned from the microfibres. 40 kHz samples were expected to be more structurally disturbed because of the mechanical effect of low frequency ultrasound. As expected, this effect was more evident in 40 kHz experiments. The surface had undergone more ruptures and the channels were disturbed at 1000 W and 2 hours exposure of ultrasound at a bath temperature of 80ºC (UST-3). This effect was tending to decrease slightly with decrease in power and bath temperature. The surface ruptures were less visible in 170 kHz treated samples though the channels were clean and smooth for all the power, temperature combinations. The majority of adsorption happens in micropores and functional groups attached to the surface of biochar (Mohan et al., 2011; Han et al., 2013). The pits cleared from the fibre attachments are more likely to be accessible for surface interactions. The breakdown of the pits and the collapses observed on the microchannels after ultrasound pre-treatments could lead to a change in surface morphology of biochar. This observation was not clearly visible in 170 kHz samples, which could be a result of lower impact bubbles by higher frequency ultrasound. Therefore, the breakdown and ruptures did not strongly occurred. The surface of 40 kHz samples seems to be very much heterogeneous, which could

affect the adsorption process. In higher frequency ultrasound, even though the microchannels were smoothened, it could happen that the surface sites were blocked because of the breaking down of microparticles or structural rearrangement.

3.2 Effect of pH and surface zeta potential

The effect of pH on adsorption properties is an important parameter to optimize because it depends on the nature of the adsorbent surface and target contaminant. The characteristics of surface functional groups on biochar changes with the pH of the solution. At low pH, most of the functional groups present on biochars are protonated and are positively charged. For $pH < pH_{pzc}$ (point of zero charge), the biochar surface is positive which favours adsorption of the anions. The presence of a large number of H^+ and H_3O^+ in the aqueous solution may compete with the cation for adsorption sites available on biochars. Thus, electrostatic repulsion will occur between cation contaminants and positively charged biochars surface thus a lower adsorption was observed at low pH in most of the studies. With the increase of pH value, the competition of metal ions and protons for binding sites decreased and more binding sites are released due to the deprotonation of functional groups. The surface of biochar is negatively charged when $pH > pH_{pzc}$. Therefore, in the higher pH range, the cations can be easily captured by biochar surface (Oh et al., 2012; Li et al., 2013).

Plot of pH against Zeta potential (Fig. 2) was examined to determine the zero-point charge and the most favourable pH condition for the solution. Ultrasound pre-treated and untreated biochar suspensions in copper solution with different pH were used to measure zeta potential.

(Figure 2 here)

Since the metal ions are positively charged (Cu^{2+}) more negative surface is favoured for adsorption. From the previous chemical characteristic studies, it was seen that the biochar we synthesized has negatively charged surface because of the acidic sites available. As seen from the plot, PZC is around 2.5 pH that means at this pH, surface is globally neutral. Any pH more than that surface will be negative. The maximum negative for the zeta potential occurred at pH 6.2. Since the copper from the solution precipitates at this pH or above (Liu et al., 2010), the optimal pH was determined as 5.5. Kołodynska et al., (2012) also had the same observation for pH in adsorption of Cu (II) from water. Therefore, for all the adsorption experiments, the pH of the solution was set in the range of 5.1 to 5.5. The results were similar for all types of biochar synthesised suggesting that the surface charge remains same after ultrasonication.

3.3 Adsorption kinetics and Statistical analysis

To understand the effect of contact time with adsorption capacity, different kinetic models were examined by fitting the experimental data to corresponding linearized kinetic models. Adsorption kinetics help to describe the physical and chemical characteristics of the biochar, which can be used to explain the surface characteristics of biochar (Lu et al., 2012; Ho and McKay, 1999).

Fig 3. shows the evolution of Cu (II) adsorption on biochar (Untreated, UST-3and UST-11 as example) with contact time. As seen in the figure, the adsorption capacity gradually increases with time until reaching a maximum value. Almost 70 percent of the adsorption occurred within 4 hours and then slowly approached the equilibrium time after 16-24 hours. The experimental data fitted only with pseudo second order model (Fig. 3, Table 3) which

was similar to the report by Mohan et al. (2007) for oak and pine wood biochars. Thus, the pseudo first order calculations were omitted.

(Figure 3 here)

Pseudo second order kinetics signified that the rate limiting mechanism is mainly by chemisorption which controls the entire adsorption process. Chemisorption involves the valence forces through the sharing or exchange of electrons between adsorbent and adsorbate and therefore the rate of desorption is considered to be negligible. 40 kHz samples showed better equilibrium adsorption capacity (Q_e) than the untreated sample. Almost 26 to 52 percent increase in Q_e values were observed among the samples. Interestingly, the adsorption on 170 kHz was less compared to 40 kHz and showed less or almost similar adsorption with the untreated sample. However, slightly better adsorption rates (k) were observed in general for the 170 kHz samples compared to untreated or 40 kHz samples.

(Table 3 here)

As evident from the kinetic data, the main driving force for the heavy metal adsorption on the surface is ionic interactions with the metal ions and surface groups. Therefore, in 170 kHz samples the only available interaction can be these ionic interactions and their specific surface area is too low for adsorptions. Nevertheless, in 40 kHz samples, in addition to the surface functional group interactions, there could be more accessibility of pores, resulting from the surface breakdowns and ruptures in the micro pits. The slight increase in equilibrium adsorption capacity can be due to this surface modification. These results are in agreement with the surface morphology observed from SEM images. As explained by He et al. (2017),

ultrasonic pre-treatments increase the exposure of the sample to the treatment solutions as well as the general accessibility of the sample, which could possibly lead to better adsorption capacity than higher frequency pre-treated samples.

To understand the effect of each ultrasonic conditions on the equilibrium adsorption capacity, statistical analysis was performed on the experimental data shown in Table 3. It was interesting to note that the ultrasonic power, bath temperature and time together affect positively towards the adsorption capacities of 40 kHz samples. The adsorption capacity is highly dependent on the combination of power with time and power with temperature (Fig.4a). In case of 170kHz samples, there was no significant trend observed (Fig. 4c). All the ultrasound conditions equally contributed to the change in adsorption capacity. The rate constant values (k) for both 40 and 170 kHz samples did not show any significant trend with pre-treatment conditions (Fig. 4b and 4d). These results also demonstrate that the low frequency ultrasound has a higher impact on equilibrium adsorption capacity of the material, yet, no appreciable effect on the speed of adsorption.

(Figure 4 here)

High frequency ultrasound, 170 kHz as in here, is not really improving to the adsorption mechanism. These samples are less preferred over untreated samples and 40 kHz as their adsorption capacity at equilibrium is not only improved but also, has been significantly decreased in some cases after ultrasound pre-treatments. The statistical analysis supports the observed fact that the ultrasound pre-treatments affect the surface properties and the low frequency ultrasound enhances the adsorption capacities of metal ions from water.

3.4 Isotherm models and Thermodynamics studies

Different adsorption isotherm models were used to describe the adsorbate-adsorbents interaction. Isotherm models were studied for the untreated biochar at maximum and minimum ultrasound pre-treatment conditions (UST-3, UST-6, UST-11 and UST-14) samples for a quick comparison of ultrasound effect. Fig 5a. is an example for the trend of change in equilibrium adsorption capacity with increase in equilibrium concentration for synthesized biochar samples (untreated,UST-3 and UST-11). Fig 5b represents the linear fitting of Freundlich model for Untreated sample, 5c and 5d shows the linear fit of Langmuir model on UST-3 and UST-11, respectively. The detailed isotherm parameters for the samples are given in Table 4. From the regression coefficient R^2, it was clearly seen that the experimental data for untreated biochar was best fit to the Freundlich isotherm, which explains the heterogeneous adsorption that is not restricted to the formation of a monolayer. The adsorption capacity increased substantially with increasing concentration with a heterogeneity factor (n) of 0.38.

(Figure 5 here)

Interestingly, for ultrasound pre-treated wood biochar, the experimental data followed Langmuir isotherm, irrespective of the ultrasound treatment condition. Langmuir model assumes monolayer adsorption of adsorbate on a homogeneous surface of adsorbent with definite number of adsorption sites having equivalent energy. A significant increase in Q_{max} was observed for UST-3 and UST-6 compared with UST-11 and UST-14, also suggesting that the low frequency ultrasound has positive effect on adsorption capacity.

(Table 4 here)

The range of value for R_L for ultrasound pre-treated samples where between 0 and 1, indicating the adsorption is favourable. As the aggressiveness of ultrasonication decreases (power, temperature and time), the value of R_L increases and approaching towards unfavourable system. This clearly indicates that the ultrasound pre-treatment favours the adsorption mechanism. Isotherm studies provided a better understanding of the fact that, ultrasound pre-treatment could possibly modify the structure of biochar and make it more homogeneous surface.

Most of the previous studies on biochar have reported that the adsorption of contaminants by biochars appeared to be an endothermic process and the adsorption capacity increased with increasing temperature (Liu and Zhang, 2009; Zhang et al., 2013; Meng et al., 2014). The enhanced temperature provides enough energy for metal ions to be captured onto the interior structure of biochar. The values of ΔH^0, ΔS^0 and ΔG^0 are used to determine thermodynamically favourable conditions for the adsorption (Al-Anber, 2011). Thermodynamic parameters where examined on the same set of samples used for isotherm studies (UST-3, UST-6, UST-11and UST-14).

For the 40 kHz samples, higher temperature was favoured with significant increase in adsorption of Cu (II). The 170 kHz samples were not following the expected trend with increase in temperature (Fig. 6) and hence the thermodynamic parameters were not calculated. The better equilibrium adsorption capacity at room temperature and decreased adsorption capacity at higher temperatures are contradicting the kinetic results of 170kHz samples. Therefore, the exact adsorption mechanism followed need to be explored further.

(Figure 6 here)

The data shown in Table 5 describe the thermodynamic parameters of selected biochar samples pre-treated at 40kHz. As seen in results, the value for ΔH^0 is positive in all the conditions indicating that the adsorption is endothermic. The positive value of ΔS^0 indicates the increase in degree of freedom or affinity at the adsorbate/adsorbent interface. This value is very low in case of UST-3 which means that there is not much structural change in adsorbent compared to others.

(Table 5 here)

The Gibb's free energy gave positive value for all the treatments, indicating that the adsorption is non-spontaneous, hence the adsorption and desorption is not in thermal equilibrium. Since the mechanism is found to be chemisorption, the adsorption is irreversible, which can be the possible explanation for positive value of ΔG^0. Similar trend was reported before for Cu (II) adsorption on hardwood biochar (Chen et al., 2011). However, the value of ΔG^0 decreased with increase in temperature, indicating that the system approaches non-spontaneous when external energy is provided. UST-3 showed almost constant ΔG^0 at all temperatures, yet the room temperature value was lesser compared with other biochar samples signifying that the adsorption on UST-3 is less non-spontaneous at room temperature and thus slightly more favourable than others. The thermodynamic results also show that the low frequency ultrasound samples are more favoured for Cu (II) adsorption compared to the untreated ones.

Isotherm and thermodynamic data were shown that the ultrasound pre-treatments have prominent effect on the adsorption behaviour of the biochar. These results also support the kinetic studies, hence motivate to assume that ultrasonic pre-treated samples can be preferred over as-synthesised untreated biochars. Mechanical effect of ultrasound plays a vital role in enhancing the surface, yet the sonochemistry behind the adsorption mechanism needs further investigation.

3.5 Comparison with Activated carbon

It was well observed that the ultrasound pre-treated biochars are exhibiting different adsorption capacity than the untreated one. Even though, the increase in adsorption capacity was not much when compared to the materials like activated carbons. Therefore, evaluating the efficiency of biochar we prepared is an important step when it is used in real life applications. Adsorption capacity per unit surface area (mg/m^2) is an interesting parameter to look in this perception (Choi et al., 2018). Table 6 represents the comparison with activated carbon and biochar we synthesised, with the BET specific surface area and corresponding equilibrium adsorption capacity Q_e. Activated carbon has an equilibrium adsorption capacity of 4.62 mg/g, for a large specific surface of 718.42 m^2/g. The value for adsorption per surface area is very less for activated carbon when compared to ultrasonic pre-treated biochar.

(Table 6 here)

Activated carbons are almost 95-99 % carbonised materials with ideally no surface functionalities attached. The only interaction with the contaminants in this case is the physisorption on surface sites by Van der Waal types of interactions. Biochar has higher

adsorption per specific surface which could be the result of chemisorption at the anchoring surface sites and modification by ultrasound. However, , high frequency pre-treated biochar exhibited better efficiency in terms of adsorption per unit surface in contrary to the initial adsorption results. Therefore, activation or chemical modifications on these biochars is of further interest to investigate the ultrasonic pre-treatment effects on chemical modifications on biochar. This could lead to a cost-effective replacement for activated carbons for heavy metal removal from water.

4. Conclusion

In this study, we aimed to investigate the physicochemical changes in biochar derived from softwood which are processed under different ultrasonic pre-treatment conditions. Kinetics, isotherm and thermodynamic studies proved that the adsorption properties of ultrasound pre-treated samples differ from untreated and enhanced properties are observed for low frequency pre-treated biochars. These results open the door to a new processing method on wood feedstock to enhance the physical properties of biochar derived from it, without changing the chemical properties. However, chemical modifications on these biochars could be interesting to provide an insight about the effect of ultrasonic pre-treatment on surface functionalisation towards adsorption capacity.

Acknowledgements

The authors gratefully acknowledge all the members of I2E3 for their great support and help during the period of this work. Financing was provided by the Natural Sciences and

Engineering Research Council of Canada (NSERC) and by Queen Elizabeth II Diamond Jubilee Scholarship.

References

1. Al-Anber, M.A. 2011. Thermodynamics approach in the adsorption of heavy metals. in: Thermodynamics-Interaction Studies-Solids, Liquids and Gases, IntechOpen.

2. Behazin, E., Ogunsona, E., Rodriguez-Uribe, A., Mohanty, A.K., Misra, M., Anyia, A.O. 2016. Mechanical, chemical, and physical properties of wood and perennial grass biochars for possible composite application. BioResources, 11(1), 1334-1348.

3. Brandes, R., Belosinschi, D., Brouillette, F., Chabot, B. 2019. A new electrospun chitosan/phosphorylated nanocellulose biosorbent for the removal of cadmium ions from aqueous solutions. J. Environ. Chem. Eng., 7(6), 103477.

4. Chen, X., Chen, G., Chen, L., Chen, Y., Lehmann, J., McBride, M.B., Hay, A.G. 2011. Adsorption of copper and zinc by biochars produced from pyrolysis of hardwood and corn straw in aqueous solution. Bioresour. Technol., 102(19), 8877-8884.

5. Chowdhury, Z.Z., Karim, M.Z., Ashraf, M.A., Khalid, K. 2016. Influence of carbonization temperature on physicochemical properties of biochar derived from slow pyrolysis of durian wood (Durio zibethinus) sawdust. BioResources, 11(2), 3356-3372.

6. Cherpozat, L., Loranger, E., Daneault, C. 2017. Ultrasonic pretreatment effects on the bio-oil yield of a laboratory-scale slow wood pyrolysis. J. Anal. Appl. Pyrolysis, 126, 31-38.

7. Choi, Y.-K., Jang, H.M., Kan, E., Wallace, A.R., Sun, W. 2018. Adsorption of phosphate in water on a novel calcium hydroxide-coated dairy manure-derived biochar. Environ. Eng. Res., 24(3), 434-442.

8. Chatterjee, R., Sajjadi, B., Mattern, D.L., Chen, W.-Y., Zubatiuk, T., Leszczynska, D., Leszczynski, J., Egiebor, N.O., Hammer, N. 2018. Ultrasound cavitation intensified amine functionalization: A feasible strategy for enhancing CO2 capture capacity of biochar. Fuel, 225, 287-298.

9. Ho, Y.-S., McKay, G. 1999. Pseudo-second order model for sorption processes. Process Biochem., 34(5), 451-465.

10. Han, Y., Boateng, A.A., Qi, P.X., Lima, I.M., Chang, J. 2013. Heavy metal and phenol adsorptive properties of biochars from pyrolyzed switchgrass and woody biomass in correlation with surface properties. J. Environ. Manage., 118, 196-204.

11. He, Z., Wang, Z., Zhao, Z., Yi, S., Mu, J., Wang, X. 2017. Influence of ultrasound pretreatment on wood physiochemical structure. Ultrason. Sonochem., 34, 136-141.

12. Inyang, M.I., Gao, B., Yao, Y., Xue, Y., Zimmerman, A., Mosa, A., Pullammanappallil, P., Ok, Y.S., Cao, X. 2016. A review of biochar as a low-cost adsorbent for aqueous heavy metal removal. Crit. Rev. Environ. Sci. Technol., 46(4), 406-433.

13. Jia, M., Wang, F., Bian, Y., Jin, X., Song, Y., Kengara, F.O., Xu, R., Jiang, X. 2013. Effects of pH and metal ions on oxytetracycline sorption to maize-straw-derived biochar. Bioresour. Technol., 136, 87-93.

14. Jindo, K., Mizumoto, H., Sawada, Y., Sanchez-Monedero, M.A., Sonoki, T. 2014. Physical and chemical characterization of biochars derived from different agricultural residues. Biogeosciences, 11(23), 6613-6621.

15. Jiang, S., Nguyen, T.A., Rudolph, V., Yang, H., Zhang, D., Ok, Y.S., Huang, L. 2017. Characterization of hard-and softwood biochars pyrolyzed at high temperature. Environ. Geochem. Health, 39(2), 403-415.

16. Kołodyńska, D., Wnętrzak, R., Leahy, J., Hayes, M., Kwapiński, W., Hubicki, Z. 2012. Kinetic and adsorptive characterization of biochar in metal ions removal. Chem. Eng. J., 197, 295-305.

17. Liu, Z., Zhang, F.-S. 2009. Removal of lead from water using biochars prepared from hydrothermal liquefaction of biomass. J. Hazard. Mater., 167(1-3), 933-939.

18. Liu, Z., Zhang, F.-S., Wu, J. 2010. Characterization and application of chars produced from pinewood pyrolysis and hydrothermal treatment. Fuel, 89(2), 510-514.

19. Leong, T., Ashokkumar, M., Kentish, S. 2011. The fundamentals of power ultrasound-A review.

20. Lu, H., Zhang, W., Yang, Y., Huang, X., Wang, S., Qiu, R. 2012. Relative distribution of Pb^{2+} sorption mechanisms by sludge-derived biochar. Water Res., 46(3), 854-862.

21. Li, M., Liu, Q., Guo, L., Zhang, Y., Lou, Z., Wang, Y., Qian, G. 2013. Cu (II) removal from aqueous solution by Spartina alterniflora derived biochar. Bioresour. Technol., 141, 83-88.

22. Loranger É., Pombert O., Drouadaine, V. 2016. Ultrasonic pre-treatments of wood chips used in a conventional pyrolysis and their effect on bio-oil composition and calorimetry. SAMPE Conference Proceedings.

23. Mohan, D., Pittman Jr, C.U., Bricka, M., Smith, F., Yancey, B., Mohammad, J., Steele, P.H., Alexandre-Franco, M.F., Gómez-Serrano, V., Gong, H. 2007. Sorption of arsenic, cadmium, and lead by chars produced from fast pyrolysis of wood and bark during bio-oil production. J. Colloid Interface Sci., 310(1), 57-73.

24. Mohan, D., Rajput, S., Singh, V.K., Steele, P.H., Pittman Jr, C.U. 2011. Modeling and evaluation of chromium remediation from water using low cost bio-char, a green adsorbent. J. Hazard. Mater., 188(1-3), 319-333.

25. Manyà, J.J. 2012. Pyrolysis for biochar purposes: a review to establish current knowledge gaps and research needs. Environ. Sci. Technol., 46(15), 7939-7954.

26. Mukome, F.N., Zhang, X., Silva, L.C., Six, J., Parikh, S.J. 2013. Use of chemical and physical characteristics to investigate trends in biochar feedstocks. J. Agric. Food Chem., 61(9), 2196-2204.

27. Meng, J., Feng, X., Dai, Z., Liu, X., Wu, J., Xu, J. 2014. Adsorption characteristics of Cu (II) from aqueous solution onto biochar derived from swine manure. Environ. Sci. Pollut. Res., 21(11), 7035-7046.

28. Mohan, D., Sarswat, A., Ok, Y.S., Pittman Jr, C.U. 2014. Organic and inorganic contaminants removal from water with biochar, a renewable, low cost and sustainable adsorbent–a critical review. Bioresour. Technol., 160, 191-202.

29. Nartey, O.D., Zhao, B. 2014. Biochar preparation, characterization, and adsorptive capacity and its effect on bioavailability of contaminants: an overview. Adv. Mater. Sci. Eng., 2014.

30. Özcan, A., Öncü, E.M., Özcan, A.S. 2006. Kinetics, isotherm and thermodynamic studies of adsorption of Acid Blue 193 from aqueous solutions onto natural sepiolite. Colloids Surf. A, 277(1-3), 90-97.

31. Oh, T.-K., Choi, B., Shinogi, Y., Chikushi, J. 2012. Effect of pH conditions on actual and apparent fluoride adsorption by biochar in aqueous phase. Water Air Soil Pollut., 223(7), 3729-3738.

32. Oliveira, F.R., Patel, A.K., Jaisi, D.P., Adhikari, S., Lu, H., Khanal, S.K. 2017. Environmental application of biochar: Current status and perspectives. Bioresour. Technol., 246, 110-122.

33. Prasad, K.K., Raheem, S. 1992. Evaluation of colour changes of indicators in the titration of cadmium with EDTA. Anal. Chim. Acta, 264(1), 137-140.

34. Peter, A., Chabot, B., Loranger, E. 2019. Enhancing Surface Properties of Softwood Biochar by Ultrasound Assisted Slow Pyrolysis. 2019 IEEE International Ultrasonics Symposium (IUS). IEEE. pp. 2477-2480.

35. Qiu, S., Wang, Z., He, Z., Yi, S. 2016. The Effect of Ultrasound Pretreatment on Poplar Wood Dimensional Stability. BioResources, 11(3), 7811-7821.

36. Sun, Y., Gao, B., Yao, Y., Fang, J., Zhang, M., Zhou, Y., Chen, H., Yang, L. 2014. Effects of feedstock type, production method, and pyrolysis temperature on biochar and hydrochar properties. Chem. Eng. J., 240, 574-578.

37. Sajjadi, B., Broome, J.W., Chen, W.Y., Mattern, D.L., Egiebor, N.O., Hammer, N., Smith, C.L. 2019. Urea functionalization of ultrasound-treated biochar: A feasible strategy for enhancing heavy metal adsorption capacity. Ultrason. Sonochem., 51, 20-30.

38. Tan, X., Liu, Y., Zeng, G., Wang, X., Hu, X., Gu, Y., Yang, Z. 2015. Application of biochar for the removal of pollutants from aqueous solutions. Chemosphere, 125, 70-85.

39. Zhang, W., Mao, S., Chen, H., Huang, L., Qiu, R. 2013. Pb (II) and Cr (VI) sorption by biochars pyrolyzed from the municipal wastewater sludge under different heating conditions. Bioresour. Technol., 147, 545-552.

40. Zhang, Z., Cao, X., Liang, P., Liu, Y. 2013. Adsorption of uranium from aqueous solution using biochar produced by hydrothermal carbonization. J. Radioanal. Nucl. Chem., 295(2), 1201-1208.

Figure captions

Figure 1: Scanning Electron Microscope images of different biochar samples (magnification 500x) a) untreated biochar b) UST-3 (40 kHz, 1000 W, 80ºC for 2 hours), c) UST-6 (40 kHz, 250 W, 20ºC for 1 hour), d) UST-11 (170 kHz, 1000 W, 80ºC for 2 hours), d) UST-14 (170 kHz, 250 W, 20ºC for 1 hour)

Figure 2: Change in zeta potential with increase in pH of the metal solution

Figure 3: Adsorption capacity of Untreated, UST-3(40 kHz, 1000 W, 80ºC for 2 hours) and UST-11 (170 kHz, 1000 W, 80ºC for 2 hours) samples with increase in contact time (top) and the pseudo second order linear plot of the experimental data (bottom)

Figure 4: Statistical correlation of ultrasonic pre-treatment conditions on equilibrium adsorption capacity, Q_e and rate constant k a) effect on Q_e of 40 kHz samples b) effect on k of 40 kHz samples c) effect on Q_e of 170 kHz samples and d) effect on k of 170 kHz samples

Fig 5. (a) Change in equilibrium adsorption capacity with concentration of metal at equilibrium (b) Freundlich isotherm model linear fitting for Untreated biochar (c) Langmuir isotherm linear fitting for UST-3 (40 kHz, 1000 W, 80oC for 2 hours) and (d) Langmuir isotherm linear fitting for UST-11 (170 kHz, 1000 W, 80oC for 2 hours)

Figure 6: Effect of temperature on equilibrium adsorption capacity of samples untreated, UST-3 (40 kHz, 1000 W, 80ºC for 2 hours) and UST-11 (170 kHz, 1000 W, 80ºC for 2 hours)

Tables and Figures

Table 1. List of ultrasonic pre-treatments on wood chips

Sample Code	Frequency (kHz)	Power (W)	Temperature (ºC)	Time (h)
UST 1	40	1000	80	1
UST 2	40	1000	20	1
UST 3	40	1000	80	2
UST 4	40	1000	20	2
UST 5	40	250	80	1
UST 6	40	250	20	1
UST 7	40	250	80	2
UST 8	40	250	20	2
UST 9	170	1000	80	1
UST 10	170	1000	20	1
UST 11	170	1000	80	2
UST 12	170	1000	20	2
UST 13	170	250	80	1
UST 14	170	250	20	1
UST 15	170	250	80	2
UST 16	170	250	20	2

Table 2. Proximate and Ultimate analyses of biochar and feedstock

Weight %	Biochar	Feedstock
Moisture	4	-
Volatile	23	-
Ash	< 1	-
C	86.5 ±1.09	46.7
H	2.7 ±0.1	6.4
N	0.05 ±0.02	0.04
O*	10.7	46.9

*Oxygen content was determined by mass balance

Table 3: Pseudo second order parameters for biochar samples

Sample	Pseudo Second order		
	Q_e (mg/g)	k (g/mg. min)	R^2
Untreated	1.09	0.051	0.9928
UST-1	1.62	0.031	0.9905
UST-2	1.59	0.017	0.9928
UST-3	1.54	0.022	0.9869
UST-4	1.38	0.015	0.9619
UST-5	1.45	0.025	0.9904
UST-6	1.6	0.068	0.9931
UST-7	1.54	0.055	0.9923
UST-8	1.66	0.020	0.9942
UST-9	0.92	0.085	0.9946
UST-10	0.98	0.080	0.9906
UST-11	0.92	0.865	0.9862
UST-12	0.79	0.321	0.9626
UST-13	0.94	0.291	0.9857
UST-14	1.42	0.015	0.9761
UST-15	0.75	0.063	0.9848
UST-16	0.78	0.179	0.9992

Table 4: Parameters of linearized Freundlich and Langmuir isotherm models for Cu adsorption on biochar

Sample	Langmuir Model				Freundlich Model		
	Q_{max}	b	R^2	R_L	K_f	n	R^2
Untreated	1.82	0.082	0.9735	0.48	5.97	0.38	0.9955
UST-3	1.62	0.091	0.9015	0.47	4.99	0.37	0.2496
UST-6	1.01	0.038	0.9988	0.71	9.71	0.41	0.9621
UST-11	1.17	0.21	0.9957	0.28	5.86	0.15	0.8541
UST-14	0.67	0.030	0.945	0.75	23.4	0.19	0.4384

Table 5: Thermodynamic parameters of copper adsorption on biochar

Sample	Temperature	Thermodynamic parameters		
	(K)	ΔG^0 (kJ/mol)	ΔH^0 (kJ/mol)	ΔS^0 (J/mol K)
Untreated	295	12.56	24.11	39.15
	313	11.85		
	333	11.07		
UST 3	295	11.51	11.63	0.43
	313	11.50		
	33	11.49		
UST 6	295	14.68	33.76	64.69
	313	13.51		
	333	12.22		

Table 6: Comparison on adsorption capacity with specific surface area

Sample	Q_e (mg/g)	Specific Surface (m^2/g)	mg/m^2
Activated carbon	4.62	718.42	0.0064
Untreated	1.09	10.48	0.104
UST-3	1.54	12.4	0.124
UST-11	0.92	3.31	0.278

Figures

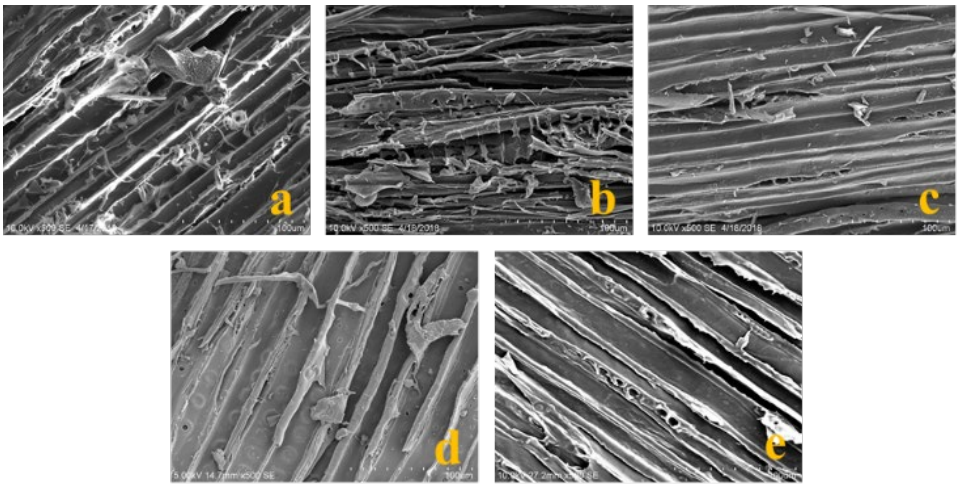

Fig 1. Scanning Electron Microscope images of different biochar samples (magnification 500x) a) untreated biochar b) UST-3 (40 kHz, 1000 W, 80 ºC for 2 hours), c) UST-6(40 kHz, 250 W, 20 ºC for 1 hour), d) UST-11(170 kHz, 1000 W, 80 ºC for 2 hours), d) UST-14(170 kHz, 250 W, 20 ºC for 1 hour)

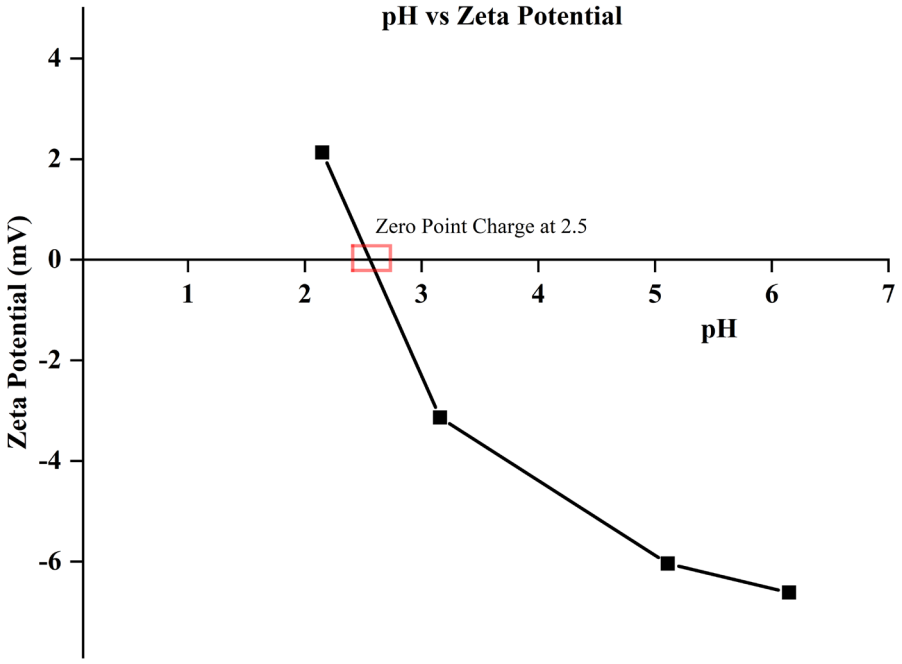

Fig 2. Change in zeta potential with increase in pH of the metal solution

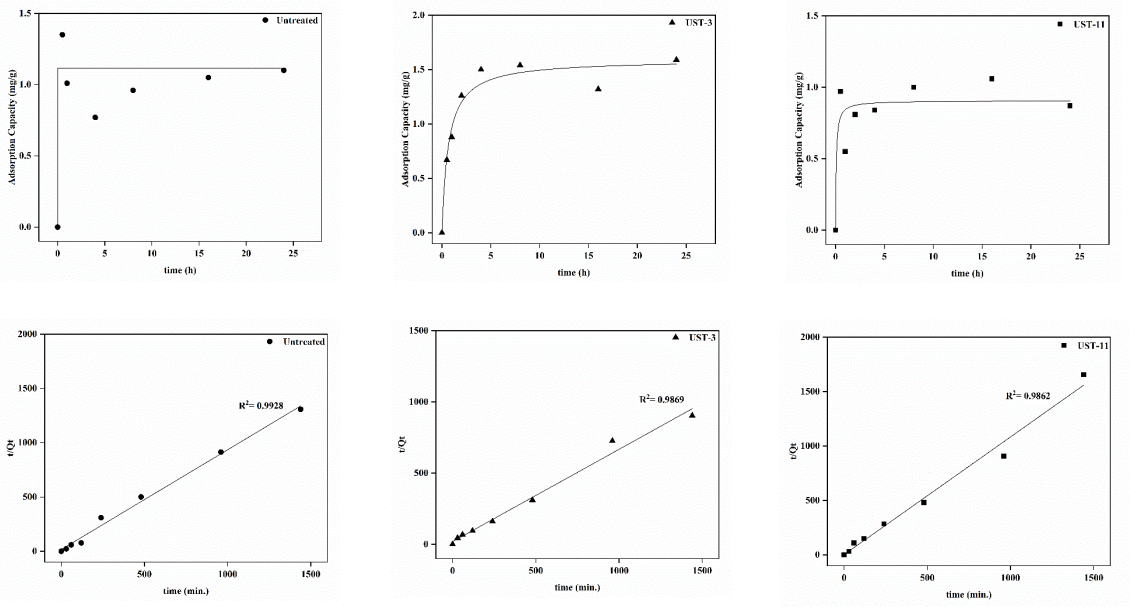

Fig 3. Adsorption capacity of Untreated, UST-3 (40 kHz, 1000 W, 80ºC for 2 hours) and UST-11 (170 kHz, 1000 W, 80ºC for 2 hours) samples with increase in contact time (top) and the pseudo second order linear plot of the experimental data (bottom)

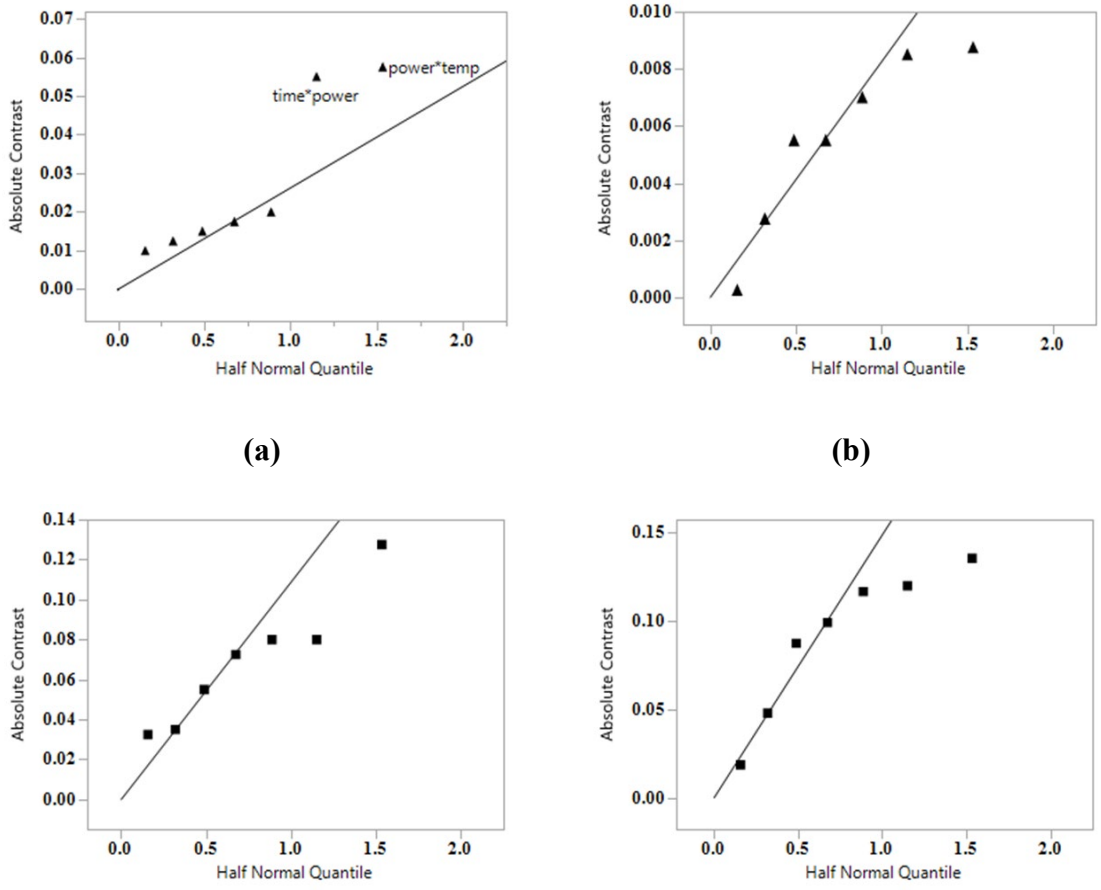

Fig 4. Statistical correlation of ultrasonic pre-treatment conditions on equilibrium adsorption capacity, Q_e and rate constant k a) effect on Q_e of 40 kHz samples b) effect on k of 40 kHz samples c) effect on Q_e of 170 kHz samples and d) effect on k of 170 kHz samples

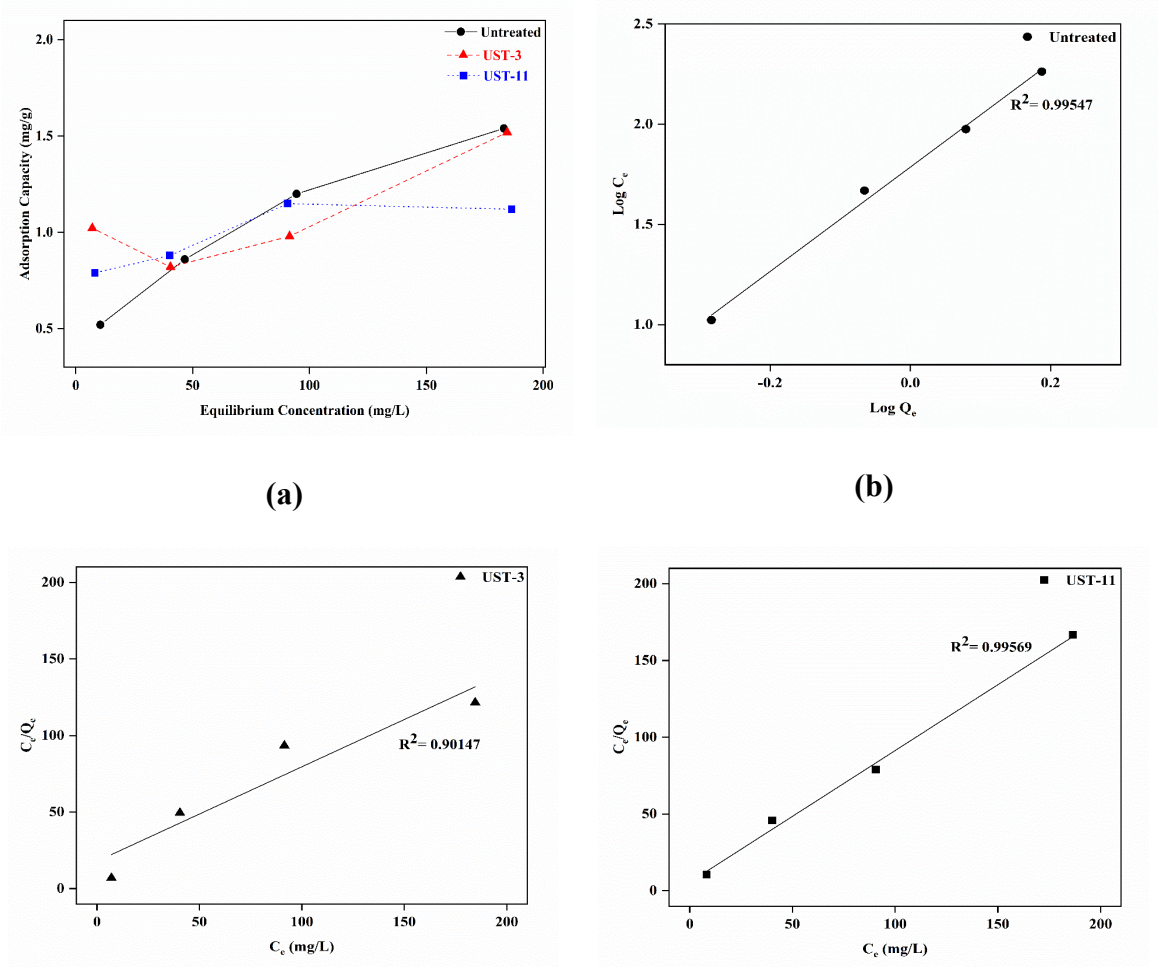

Fig 5. (a) Change in equilibrium adsorption capacity with concentration of metal at equilibrium (b) Freundlich isotherm model linear fitting for Untreated biochar (c) Langmuir isotherm linear fitting for UST-3 (40 kHz, 1000 W, 80ºC for 2 hours) and (d) Langmuir isotherm linear fitting for UST-11 (170 kHz, 1000 W, 80ºC for 2 hours)

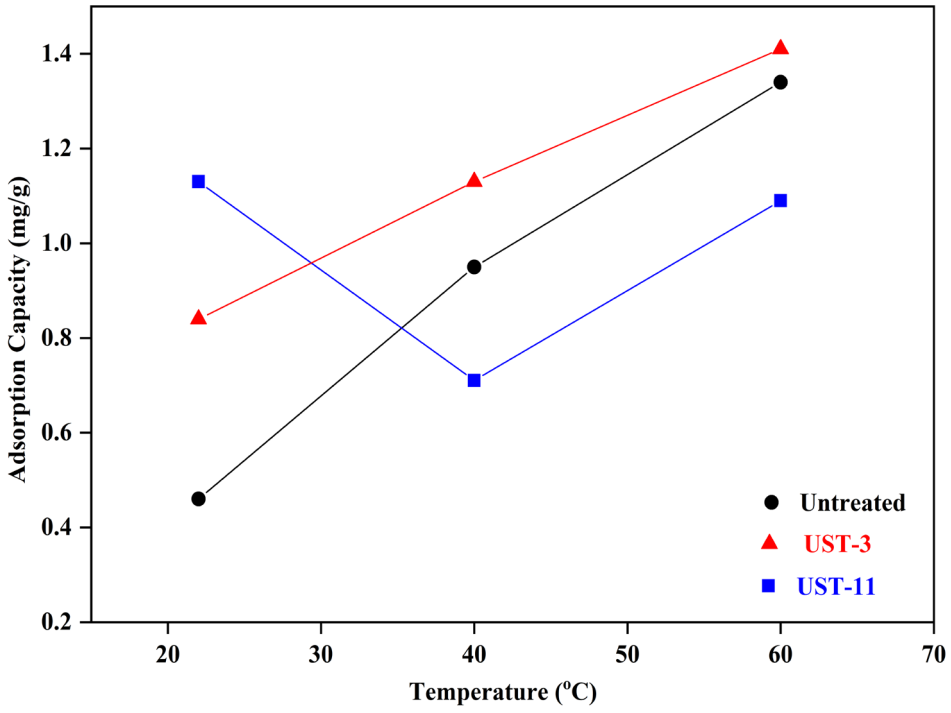

Fig 6. Effect of temperature on equilibrium adsorption capacity of samples untreated, UST-3 (40 kHz, 1000 W, 80°C for 2 hours) and UST-11(170 kHz, 1000 W, 80°C for 2 hours)